

Performance Comparison of Numerical Optimization Algorithms for RSS-TOA-Based Target Localization

Halim Lee
School of Integrated Technology
Yonsei University
Incheon, Korea
halim.lee@yonsei.ac.kr

Jiwon Seo
School of Integrated Technology
Yonsei University
Incheon, Korea
jiwon.seo@yonsei.ac.kr

Abstract—In the literature, a hyper-enhanced local positioning system (HELPS) was developed to locate a target mobile device in an emergency. HELPS finds the target mobile device (i.e., emergency caller) using multiple receivers (i.e., signal measurement equipment of first responders) that measure the received signal strength (RSS) and time of arrival (TOA) of the long-term evolution (LTE) uplink signal from the target mobile device. The maximum likelihood (ML) estimator can be applied to localize a target mobile device using the RSS and TOA. However, the ML estimator for the RSS-TOA-based target localization problem is nonconvex and nonlinear, having no analytical solution. Therefore, the ML estimator should be solved numerically, unless it is relaxed into a convex or linear form. This study investigates the target localization performance and computational complexity of numerical methods for solving an ML estimator. The three widely used numerical methods are: grid search, gradient descent, and particle swarm optimization. In the experimental evaluation, the grid search yielded the lowest target localization root-mean-squared error; however, the 95th percentile error of the grid search was larger than those of the other two algorithms. The average code computation time of the grid search was extremely large compared with those of the other two algorithms, and gradient descent exhibited the lowest computation time. HELPS can select numerical algorithms by considering their constraints (e.g., the computational resources of the localization server or target accuracy).

Index Terms—Target Localization, Numerical Algorithms, Emergency Response, E911 Positioning.

I. INTRODUCTION

Target localization (i.e., passive target localization or passive emitter localization) [1]–[10] is widely used in mission-critical applications, such as asset localization, wireless sensor networks, and search and rescue; target localization refers to the estimation of the location of a target device that transmits a wireless signal using a single or multiple receivers.

In an emergency response (e.g., “911 emergency”), the target localization technologies are especially helpful in localizing the emergency caller. Currently, several regions, such as the United States (U.S.A) and Europe, require mobile service providers to provide position information on the target mobile device in the emergency situations [11], [12].

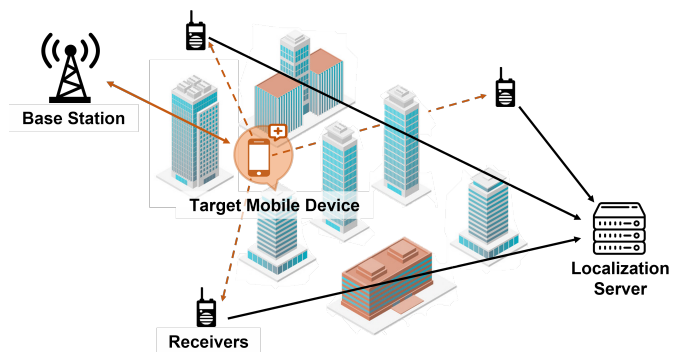


Fig. 1. Operational concept of HELPS.

In open-sky environments, the meter-level position information of the target mobile device can be provided using a global navigation satellite system (GNSS) [13]–[15], such as global positioning service (GPS) of the U.S.A, GLONASS of Russia, and Galileo of Europe. However, in harsh signal environments, such as dense urban, indoor, and tunnel environments, the accuracy and availability of GNSS-based positioning rapidly decrease because of signal blockage or reflection [16]–[25]. Further, GNSS signal is vulnerable to malicious jamming [26]–[32] or ionospheric anomalies [33]–[37].

Target localization can be used as an alternative positioning method in such environments. Recently, researchers in South Korea have developed a positioning system for emergency responses called the hyper-enhanced local positioning system (HELPS) [38], [39], which applies the concept of target localization to its positioning algorithm.

Fig. 1 shows the operational concept of the HELPS, which has four main components: a target mobile device, receivers (i.e., signal measurement equipment (MSE)), localization server (i.e., location calculation server (LCS)), and base station.

When a target mobile device makes an emergency call, the emergency control center roughly identifies the position of the target mobile device using less accurate positioning

methods (e.g., single-cellular-tower based localization) [40]–[42]. Subsequently, the first responders are dispatched to the emergency site, and a long-term evolution (LTE) uplink signal, transmitted from the target mobile device using receivers, is measured. These signal measurements are transmitted to a localization server, which estimates the position of the target mobile device. This study focuses on the positioning algorithm of HELPS, which is performed out of the localization server. Further details on HELPS can be found in [38], [39].

Among several signal measurements, such as the received signal strength (RSS) [1]–[10], channel impulse response (CIR) [43], [44] and time-of-arrival (TOA) [1]–[4], this study assumes that receivers can measure the RSS and TOA because they can be obtained using relatively portable receivers.

Maximum likelihood estimation (MLE) [5]–[10] can be applied to calculate the position of a target mobile device using both the RSS and TOA measurements. However, the cost function of MLE for RSS-TOA-based target localization is nonconvex and nonlinear. As the cost function of MLE has no closed-form solution, it cannot be solved analytically.

Previous studies [1]–[5] proposed various optimization methods to obtain optimal or suboptimal solutions, and they considered wireless signal networks (WSNs) that have limited computational resources. Therefore, they relaxed the original maximum likelihood (ML) estimator to a closed-form estimator, which can potentially lower the target localization performance when the RSS error is large.

This study simulates the emergency situations wherein the target must be precisely located, even if a relatively large amount of computational resources is required on the localization server. Therefore, numerical algorithms were considered to find the optimal solution without relaxation of the ML estimator.

The three popular numerical algorithms are grid search [9], [10], gradient descent [45], [46], and particle swarm optimization (PSO) [47], [48]. These are well-used algorithms, but their performances in the TOA-RSS-based target localization problem have not been evaluated in the literature. Therefore, this study experimentally evaluated the target localization performance and computation time of three algorithms for the RSS-TOA-based target localization problem.

The remainder of this paper is organized as follows. Section II describes the RSS-TOA-based target localization problem and maximum likelihood (ML) estimator. Section III briefly describes the three optimization methods used in this study: grid search, gradient descent, and PSO. Section IV introduces the experimental settings for evaluation and Section V discusses the experimental results. Finally, Section VI concludes the paper.

II. PROBLEM DESCRIPTION

A. RSS and TOA Measurements

When a total of N receivers are dispatched to the emergency site, the RSS P_i (dBm) measured by the i -th receiver can be modeled as a log-normal path loss model [5]–[7], [9].

$$\begin{aligned} P_i &= P_0 - 10\beta \log_{10} \frac{d_i}{d_0} + n_{\text{RSS},i}, \\ d_i &= \|\mathbf{x} - \mathbf{r}_i\|, \\ n_i &\sim \mathcal{N}(0, \sigma_{\text{dB}}^2), \end{aligned} \quad (1)$$

where P_0 (dBm) is the signal power at the reference distance d_0 from the target (d_0 is set to 1 m in this study); β is the path loss exponent; $n_{\text{RSS},i}$ is the log-normal shadowing term which is modeled as a zero-mean normal distribution with a standard deviation of σ_{RSS} (dB); $\mathbf{x} = [x_t, y_t]^T$ is the 2D position of the target mobile device; $\mathbf{r}_i = [x_{r_i}, y_{r_i}]^T$ is the 2D position of i -th receiver; and $\|\cdot\|$ denotes L^2 norm.

The TOA T_i (s) is measured by the i -th receiver, which can be modeled as

$$T_i = \frac{d_i}{c} + \tau + n_{\text{TOA},i}, \quad (2)$$

where c is the speed of light; τ is the clock bias of the target mobile device; and $n_{\text{TOA},i}$ is the random noise term which is modeled as a normal distribution with a standard deviation of σ_{TOA} (s).

B. Maximum Likelihood Estimator

In Eqs. (1) and (2), four unknowns should be estimated: x_t , y_t , P_0 , and τ . The ML estimator for estimating the unknowns, $\boldsymbol{\theta} = [\mathbf{x}^T, P_0, \tau]^T = [x_t, y_t, P_0, \tau]^T$, is given by

$$\begin{aligned} \hat{\boldsymbol{\theta}} &= \arg \min_{\boldsymbol{\theta}} F(\boldsymbol{\theta}) \\ &= \arg \min_{\boldsymbol{\theta}} \sum_i^N \left\{ (P_i - P_0 + 10\beta \log_{10} d_i)^2 \right. \\ &\quad \left. + w \cdot (T_i - d_i/c - \tau)^2 \right\}, \end{aligned} \quad (3)$$

where w is a weighting factor that considers the scale of RSS and TOA errors. In this study, we empirically set the weighting factor as $w = 4 \cdot 10^{-5} d_i - 10^{-3}$.

As previously mentioned, the ML estimator in Eq. (3) has no closed-form solution. Therefore, the ML estimator in Eq. (3) should be solved numerically.

III. OPTIMIZATION ALGORITHMS

This section briefly introduces the three optimization algorithms used to obtain the numerical solution of Eq. (3).

A. Grid Search

Grid search [9], [10] is a brute-force search, which finds the optimal solution that minimizes cost after sequentially evaluating every combination of parameters (i.e., candidate solutions). The candidate solutions of the grid search are determined within the search space and at search interval. The closer the search interval, the more accurate is the optimal solution; however, more computation time is required. A grid search is a simple and high-performance method that is computationally inefficient.

B. Gradient Descent

Gradient descent (i.e., steepest descent) [45], [46] is an iterative algorithm that determines the local minimum by traveling forward in the opposite direction to the gradient. Starting with the initial guess of the parameters θ_0 , the next guess θ_{k+1} ($k = 0, 1, 2, \dots$) is updated as follows [46]:

$$\theta_{k+1} = \theta_k - \gamma \cdot \nabla F(\theta_k), \quad (4)$$

where $\gamma \in \mathbb{R}_+$ is the learning rate; and $\nabla F(\cdot)$ denotes the gradient of function F . If the learning rate γ is set properly, $F(\theta)$ decreases gradually (i.e., $F(\theta_k) \geq F(\theta_{k+1})$).

C. Particle Swarm Optimization

PSO [47], [48] is a population-based algorithm that determines the optimal solution by improving multiple candidate solutions (i.e., particles). In every iteration, particles iteratively move to their local best position. The final PSO solution has the lowest cost among the candidate solutions. Because each agent optimizes its own position by exchanging information, it is expected to find the global minimum, even if some agents fall into the local minimum.

The PSO algorithm used in this study is implemented as shown in Algorithm 1. The maximum number of iterations is denoted as M and total number of particles is denoted as S . $\mathbf{b}_{\text{lower}}$ and $\mathbf{b}_{\text{upper}}$ are the lower and upper bounds on the parameters, respectively. The final output of the algorithm is the best solution θ_{best} . Given the lower and upper bounds, the PSO algorithm initializes the population using a uniform distribution, and the velocity matrix is also randomly initialized. At every epoch, the PSO algorithm updates the velocity of each particle, considering the best solution of the i -th particle (i.e., p_i) and best solution of the entire population (i.e., θ_{best}). w , c_1 , and c_2 are weights of each term that update the velocity. After updating the position of the particle θ_i , p_i or θ_{best} can be updated if θ_i has a lower cost compared with the current best solution.

IV. EXPERIMENTAL SETTINGS

Fig. 2 shows the experimental environment near the Seongdong Bridge, Seoul, South Korea. The target mobile device was placed below the bridge, as indicated by the red phone icon. Four signal collection points, 50, 100, 150, and 200 m from the target mobile device, are indicated by the yellow person icons. The RSS and TOA were measured 90 times at each signal-collection point. A Samsung Galaxy S8+ was used as the mobile device, Xilinx XCKU9P 1FFVE900I was used as the receiver, and field-programmable gate array (FPGA) board was programmed to measure the RSS and TOA of the signal transmitted from the target mobile device [38], [39]. The central frequency of the signal was set to 738 MHz, and bandwidth was set to 10 MHz.

In the grid search, the search space for \mathbf{x} was set to twice the distance between the target mobile device and receiver (i.e., the search space was set to 100, 200, 300, and 400 m for each experimental setting in Fig. 2). The search interval

Algorithm 1: PSO algorithm for estimating the best solution θ_{best}

Data: F , M , S , $\mathbf{b}_{\text{lower}}$, $\mathbf{b}_{\text{upper}}$
Result: θ_{best}
 Randomly initialize the population
 $\mathcal{P} = [\theta_1, \theta_2, \dots, \theta_S]$ within $[\mathbf{b}_{\text{lower}}, \mathbf{b}_{\text{upper}}]$
 Randomly initialize the velocity $\mathcal{V} = [v_1, v_2, \dots, v_S]$
for $iter \in 1, 2, \dots, M$ **do**
 for $i \in 1, 2, \dots, S$ **do**
 Pick random numbers r_1, r_2 within $[0, 1]$
 $v_i \leftarrow w \cdot v_i + c_1 \cdot r_1 \cdot (p_i - \theta_i) + c_2 \cdot r_2 \cdot (\theta_{\text{best}} - \theta_i)$
 $\theta_i \leftarrow \theta_i + v_i$
 if $F(\theta_i) < F(p_i)$ **then**
 $p_i \leftarrow \theta_i$
 if $F(p_i) < F(\theta_{\text{best}})$ **then**
 $\theta_{\text{best}} \leftarrow p_i$
 end
 end
 end
end
return θ_{best}

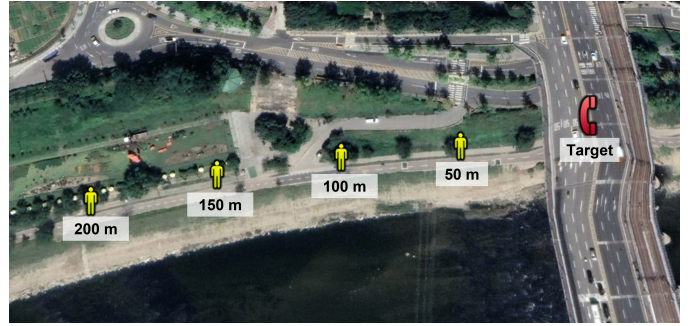


Fig. 2. Experimental environment.

was set at 1 m. The search space and search interval for $P0$ were set to 6 and 0.5 dB, respectively. The search space and search interval for $c \cdot \tau$ were set to 50 and 5 m, respectively. The initial values of parameters were obtained by semidefinite programming (SDP) in [5]. The learning rate of the gradient descent was set to 0.001. The initial guess of the parameters was set as $\theta_0 = [x_t - 20, y_t - 20, -60, 1350]^T$. The total iteration of the gradient descent was set to 200. In the PSO, M was set to 200 and S was set to 100. The weights w , c_1 , and c_2 were set to 0.8, 0.1, and 0.1, respectively. The lower and upper bounds (b_{lower} and b_{upper}) were set as in the search space of the grid search.

Algorithms were programmed in Python and ran on a desktop with an Intel Core i7-8700 CPU operating at 3.20 GHz and 16 GB of memory.

V. EXPERIMENTAL RESULTS

A. Performance Comparison of Three Algorithms

Fig. 3 shows a 2D plot and cumulative distribution function (CDF) of the target localization errors of the three algorithms.

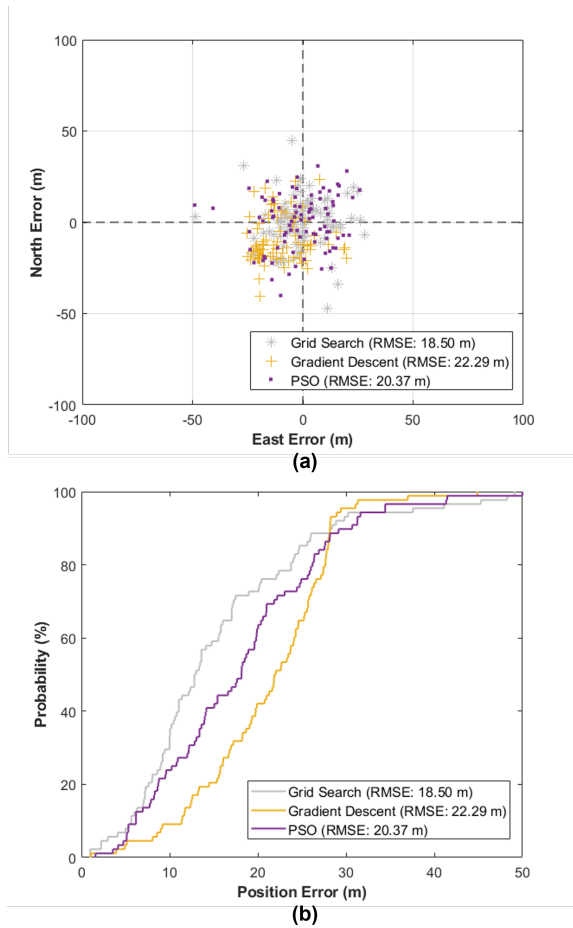


Fig. 3. (a) 2D target localization error and (b) cumulative localization error distribution of the three algorithms.

For the evaluation, it was assumed that the four receivers were placed evenly around the target mobile device. The root mean square errors (RMSE) of the grid search, gradient descent, and PSO algorithms are 18.50, 22.29, and 20.37 m, respectively. When comparing the RMSE, the grid search showed better performance than the other two algorithms.

Table I compares the 80th and 95th percentiles of the target localization errors for the three algorithms. In emergencies, it is important to estimate the locations of emergency callers without omissions. Therefore, ensuring a specific level of target localization accuracy for strict criteria, such as 80% or 95%, is necessary. When comparing the 95th percentile error, grid search showed poor performance compared with gradient descent or PSO. However, we assumed that the initial estimate was fairly close to the global minimum (i.e., the initial estimate was approximately 28.3 m away from the global minimum) in the gradient descent algorithm. Therefore, the performance of gradient descent is expected to worsen if the initial guess is far from the global minimum.

B. Comparison of Computation Time

Fig. 4 compares the average code computation times of the three algorithms. The grid search is computationally inefficient

TABLE I
PERFORMANCE COMPARISON AMONG THREE ALGORITHMS (UNIT: M)

	Grid Search	Gradient Descent	PSO
80%	23.77	27.65	26.20
95%	37.58	29.40	34.43

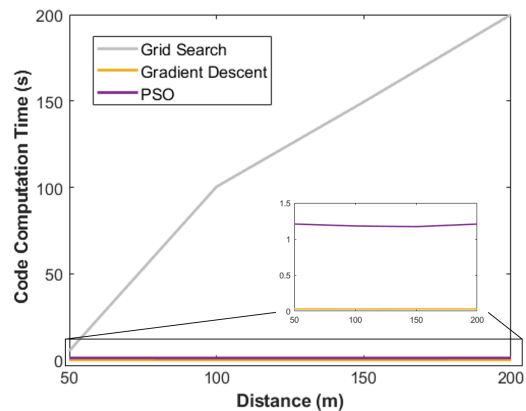


Fig. 4. Average code computation time of the three algorithms.

compared with the other two algorithms. As the search space increased (i.e., the distance between the target and receiver increased), the code computation time increased significantly. The computation time of the grid search can be reduced by increasing the search interval and decreasing the search space; however, there is a risk of increasing the target localization error. In the case of PSO, the computation time can be reduced by reducing the number of particles and total epochs.

VI. CONCLUSION

This study solved the nonconvex and nonlinear ML estimators for RSS-TOA-based target localization and considered three numerical methods for solving the ML estimator: grid search, gradient descent, and PSO. We experimentally evaluated the target localization performances and computational complexities of the three algorithms. The target localization RMSE decreases in the following order: grid search, PSO, and gradient descent. However, the 95th percentile error of the grid search was larger than those of the other two methods. The average code computation time increases in the following order: grid search, PSO, and gradient descent. The grid search was computationally inefficient compared with the other two algorithms.

ACKNOWLEDGMENT

The authors would like to thank the Communication System Laboratory of Hanyang University, Korea, for the data collection. This research was supported in part by the Institute of Information & Communications Technology Planning & Evaluation (IITP) grant funded by the Korea government

(KNPA) (2019-0-01291); in part by the Future Space Navigation & Satellite Research Center through the National Research Foundation funded by the Ministry of Science and ICT, Republic of Korea (2022M1A3C2074404); and in part by the Unmanned Vehicles Core Technology Research and Development Program through the National Research Foundation of Korea (NRF) and the Unmanned Vehicle Advanced Research Center (UVARC) funded by the Ministry of Science and ICT, Republic of Korea (2020M3C1C1A01086407).

REFERENCES

- [1] S. Tomic and M. Beko, "A robust NLOS bias mitigation technique for RSS-TOA-based target localization," *IEEE Signal Process. Lett.*, vol. 26, no. 1, pp. 64–68, 2019.
- [2] M. Katwe, P. Ghare, P. K. Sharma, and A. Kothari, "NLOS error mitigation in hybrid RSS-TOA-based localization through semi-definite relaxation," *IEEE Commun. Lett.*, vol. 24, no. 12, pp. 2761–2765, 2020.
- [3] Y. Wang, F. Zheng, M. Wiemeler, W. Xiong, and T. Kaiser, "Reference selection for hybrid TOA/RSS linear least squares localization," in *Proc. IEEE VTC*, 2013, pp. 1–5.
- [4] K. Panwar, M. Katwe, P. Babu, P. Ghare, and K. Singh, "A majorization-minimization algorithm for hybrid TOA-RSS based localization in NLOS environment," *IEEE Commun. Lett.*, vol. 26, no. 5, pp. 1017–1021, 2022.
- [5] R. M. Vaghefi, M. R. Gholami, R. M. Buehrer, and E. G. Strom, "Cooperative received signal strength-based sensor localization with unknown transmit powers," *IEEE Trans. Signal Process.*, vol. 66, no. 4, pp. 3197–3210, 2016.
- [6] R. W. Ouyang, A. K. Wong, and C. Lea, "Received signal strength-based wireless localization via semidefinite programming: Noncooperative and cooperative schemes," *IEEE Trans. Veh. Technol.*, vol. 59, no. 3, pp. 1307–1318, 2010.
- [7] X. Li, "Collaborative localization with received-signal strength in wireless sensor networks," *IEEE Trans. Veh. Technol.*, vol. 56, no. 6, pp. 3807–3817, 2007.
- [8] S. Jeong, H. Lee, T. Kang, and J. Seo, "RSS-based LTE base station localization using single receiver in environment with unknown path-loss exponent," in *Proc. ICTC*, 2020, pp. 958–961.
- [9] H. Lee, T. Kang, S. Jeong, and J. Seo, "Evaluation of RF fingerprinting-aided RSS-based target localization for emergency response," in *Proc. IEEE VTC*, Jun. 2022, pp. 1–7.
- [10] H. Lee and J. Seo, "Performance evaluation and hybrid application of the greedy and predictive UAV trajectory optimization methods for localizing a target mobile device," in *Proc. ION ITM*, Jan. 2023, pp. 161–171.
- [11] Federal Communications Commission, "Wireless E911 location accuracy requirements," FCC 19-124A1, Nov. 2019.
- [12] European Commission, "Radio equipment directive," Directive 2014/53/EU, Apr. 2014.
- [13] P. Misra and P. K. Enge, *The Global Positioning System: Signals, Measurements, and Performance*. Ganga-Jamuna Press, 1994.
- [14] P. Dabove and V. D. Pietra, "Towards high accuracy GNSS real-time positioning with smartphones," *Adv. Space Res.*, vol. 63, no. 1, pp. 94–102, 2019.
- [15] H. Yoon, H. Seok, C. Lim, and B. Park, "An online SBAS service to improve drone navigation performance in high-elevation masked areas," *Sensors*, vol. 20, no. 11, p. 3047, 2020.
- [16] H. Lee, J. Seo, and Z. Kassas, "Urban road safety prediction: A satellite navigation perspective," *IEEE Intell. Transp. Syst. Mag.*, vol. 14, no. 6, pp. 94–106, Nov.-Dec. 2022.
- [17] N. Agarwal, J. Basch, P. Beckmann, P. Bharti, S. Bloebaum, S. Casadei, A. Chou, P. Enge, W. Fong, N. Hathi, and W. Mann, "Algorithms for GPS operation indoors and downtown," *GPS Solut.*, vol. 6, no. 3, pp. 149–160, 2002.
- [18] Y. Lee and B. Park, "Nonlinear regression-based GNSS multipath modelling in deep urban area," *Mathematics*, vol. 10, no. 3, p. 412, 2022.
- [19] H. Lee, T. Kang, and J. Seo, "Safety distance visualization tool for LTE-based UAV positioning in urban areas," *J. Adv. Navig. Technol.*, vol. 23, no. 5, pp. 408–414, 2019.
- [20] S. Kim, H. Lee, and K. Park, "GPS multipath detection based on carrier-to-noise-density ratio measurements from a dual-polarized antenna," in *Proc. ICCAS*, 2021, pp. 1099–1103.
- [21] J. Kim, J.-W. Kwon, and J. Seo, "Multi-UAV-based stereo vision system without GPS for ground obstacle mapping to assist path planning of UGV," *Electron. Lett.*, vol. 50, no. 20, pp. 1431–1432, Sep. 2014.
- [22] T. Kang and J. Seo, "Practical simplified indoor multiwall path-loss model," in *Proc. ICCAS*, 2020, pp. 774–777.
- [23] H. Lee and J. Seo, "Performance comparison of machine learning algorithms for received signal strength-based indoor LOS/NLOS classification of LTE signals," *J. Position. Navig. Timing*, vol. 11, no. 4, pp. 361–368, 2022.
- [24] M. Jia, H. Lee, J. Khalife, Z. M. Kassas, and J. Seo, "Ground vehicle navigation integrity monitoring for multi-constellation GNSS fused with cellular signals of opportunity," in *Proc. IEEE ITSC*, 2021, pp. 3978–3983.
- [25] H. Lee, J. Seo, and Z. Kassas, "Integrity-based path planning strategy for urban autonomous vehicular navigation using GPS and cellular signals," in *Proc. ION GNSS+*, 2020, pp. 2347–2357.
- [26] K. Park, D. Lee, and J. Seo, "Dual-polarized GPS antenna array algorithm to adaptively mitigate a large number of interference signals," *Aerosp. Sci. Technol.*, vol. 78, pp. 387–396, Jul. 2018.
- [27] K. Park and J. Seo, "Single-antenna-based GPS antijamming method exploiting polarization diversity," *IEEE Trans. Aerosp. Electron. Syst.*, vol. 57, no. 2, pp. 919–934, Apr. 2021.
- [28] W. Kim, P.-W. Son, J. Rhee, and J. Seo, "Development of record and management software for GPS/Loran measurements," in *Proc. ICCAS*, 2020, pp. 796–799.
- [29] W. Kim, P.-W. Son, S. G. Park, S. H. Park, and J. Seo, "First demonstration of the Korean eLoran accuracy in a narrow waterway using improved ASF maps," *IEEE Trans. Aerosp. Electron. Syst.*, vol. 58, no. 2, pp. 1492–1496, Apr. 2022.
- [30] J. Park, P.-W. Son, W. Kim, J. Rhee, and J. Seo, "Effect of outlier removal from temporal ASF corrections on multichain Loran positioning accuracy," in *Proc. ICCAS*, 2020, pp. 824–826.
- [31] J. H. Rhee, S. Kim, P.-W. Son, and J. Seo, "Enhanced accuracy simulator for a future Korean nationwide eLoran system," *IEEE Access*, vol. 9, pp. 115 042–115 052, Aug. 2021.
- [32] S. Lee, E. Kim, and J. Seo, "SFOL DME pulse shaping through digital predistortion for high-accuracy DME," *IEEE Trans. Aerosp. Electron. Syst.*, vol. 58, no. 3, pp. 2616–2620, June 2022.
- [33] H. Lee, S. Pullen, J. Lee, B. Park, M. Yoon, and J. Seo, "Optimal parameter inflation to enhance the availability of single-frequency GBAS for intelligent air transportation," *IEEE Trans. Intell. Transp. Syst.*, vol. 23, no. 10, pp. 17 801–17 808, Oct. 2022.
- [34] A. K. Sun, H. Chang, S. Pullen, H. Kil, J. Seo, Y. J. Morton, and J. Lee, "Markov chain-based stochastic modeling of deep signal fading: Availability assessment of dual-frequency GNSS-based aviation under ionospheric scintillation," *Space Weather*, vol. 19, no. 9, pp. 1–19, Sep. 2021.
- [35] M. Yoon and J. Lee, "Medium-scale traveling ionospheric disturbances in the Korean region on 10 November 2004: Potential impact on GPS-based navigation systems," *Space Weather*, vol. 12, no. 4, pp. 173–186, 2014.
- [36] J. Lee, Y. Morton, J. Lee, H.-S. Moon, and J. Seo, "Monitoring and mitigation of ionospheric anomalies for GNSS-based safety critical systems," *IEEE Signal Process. Mag.*, vol. 34, no. 5, pp. 96–110, Sep. 2017.
- [37] E. Bang and J. Lee, "Methodology of automated ionosphere front velocity estimation for ground-based augmentation of GNSS," *Radio Sci.*, vol. 48, no. 6, pp. 659–670, 2013.
- [38] H. Moon, H. Park, and J. Seo, "HELPS for emergency location service: Hyper-enhanced local positioning system," *IEEE Intell. Transp. Syst. Mag.*, 2023, in preparation.
- [39] S. Min and H. Moon, "Detection range of signal measurement equipment in HELPS," in *Proc. IEEE VTC*, Jun. 2022, pp. 1–5.
- [40] Y. Zhao, "Standardization of mobile phone positioning for 3G systems," *IEEE Commun. Mag.*, vol. 40, no. 7, pp. 108–116, 2002.
- [41] E. Tsalolikhin, I. Bilik, and N. Blaunstein, "A single-base-station localization approach using a statistical model of the NLOS propagation conditions in urban terrain," *IEEE Trans. Veh. Technol.*, vol. 60, no. 3, pp. 1124–1137, 2011.

- [42] M. Vossiek, L. Wiebking, P. Gulden, J. Wieghardt, C. Hoffmann, and P. Heide, "Wireless local positioning," *IEEE Microw. Mag.*, vol. 4, no. 4, pp. 77–86, 2003.
- [43] H. Lee and J. Seo, "A preliminary study of machine-learning-based ranging with LTE channel impulse response in multipath environment," in *Proc. IEEE ICCE-Asia*, 2020.
- [44] H. Lee, A. Abdallah, J. Park, J. Seo, and Z. Kassas, "Neural network-based ranging with LTE channel impulse response for localization in indoor environments," in *Proc. ICCAS*, 2020, pp. 939–944.
- [45] P. Baldi, "Gradient descent algorithm overview: A general dynamical systems perspective," *IEEE Trans. Neural Netw. Learn. Syst.*, vol. 6, no. 1, pp. 181–195, 1995.
- [46] S. Ruder, "An overview of gradient descent optimization algorithms," *arXiv preprint arXiv:1609.04747*, 2016.
- [47] R. V. Kulkarni and G. K. Venayagamoorthy, "Particle swarm optimization in wireless-sensor networks: A brief survey," *IEEE Trans. Syst. Man. Cybern. C Appl. Rev.*, vol. 41, no. 2, pp. 262–267, 2010.
- [48] J. R. Parvin and C. Vasanthanayaki, "Particle swarm optimization-based energy efficient target tracking in wireless sensor network," *Measure.*, vol. 147, p. 106882, 2019.